Eur. Phys. J. A **30**, 471–476 (2006)
DOI 10.1140/epja/i2006-10162-1

THE EUROPEAN PHYSICAL JOURNAL A

Letter

Lowest-Q^2 measurement of the $\gamma^*p \to \Delta$ reaction: Probing the pionic contribution

The A1 Collaboration

S. Stave[1,a], M.O. Distler[2], I. Nakagawa[1,3,b], N. Sparveris[4], P. Achenbach[2], C. Ayerbe Gayoso[2], D. Baumann[2], J. Bernauer[2], A.M. Bernstein[1,c], R. Böhm[2], D. Bosnar[5], T. Botto[1], A. Christopoulou[4], D. Dale[3], M. Ding[2], L. Doria[2], J. Friedrich[2], A. Karabarbounis[4], M. Makek[5], H. Merkel[2], U. Müller[2], R. Neuhausen[2], L. Nungesser[2], C.N. Papanicolas[4], A. Piegsa[2], J. Pochodzalla[2], M. Potokar[6], M. Seimetz[2,d], S. Širca[6], S. Stiliaris[4], Th. Walcher[2], and M. Weis[2]

[1] Department of Physics, Laboratory for Nuclear Science and Bates Linear Accelerator Center, Massachusetts Institute of Technology, Cambridge, MA 02139, USA
[2] Institut für Kernphysik, Johannes Gutenberg-Universität Mainz, D-55099 Mainz, Germany
[3] Department of Physics and Astronomy, University of Kentucky, Lexington, KY 40206, USA
[4] Institute of Accelerating Systems and Applications and Department of Physics, University of Athens, Athens, Greece
[5] Department of Physics, University of Zagreb, Croatia
[6] Institute Jožef Stefan, University of Ljubljana, Ljubljana, Slovenia

Received: 21 September 2006 / Revised: 5 December 2006 /
Published online: 22 December 2006 –
Communicated by M. Garçon

Abstract. To determine nonspherical angular-momentum amplitudes in hadrons at long ranges (low Q^2), data were taken for the $p(\vec{e},e'p)\pi^0$ reaction in the Δ region at $Q^2 = 0.060$ $(\mathrm{GeV}/c)^2$ utilizing the magnetic spectrometers of the A1 Collaboration at MAMI. The results for the dominant transition magnetic dipole amplitude and the quadrupole to dipole ratios at $W = 1232$ MeV are $M_{1+}^{3/2} = (40.33 \pm 0.63_{\mathrm{stat+syst}} \pm 0.61_{\mathrm{model}})(10^{-3}/m_{\pi^+})$, $\mathrm{Re}(E_{1+}^{3/2}/M_{1+}^{3/2}) = (-2.28 \pm 0.29_{\mathrm{stat+syst}} \pm 0.20_{\mathrm{model}})\%$, and $\mathrm{Re}(S_{1+}^{3/2}/M_{1+}^{3/2}) = (-4.81 \pm 0.27_{\mathrm{stat+syst}} \pm 0.26_{\mathrm{model}})\%$. These disagree with predictions of constituent quark models but are in reasonable agreement with lattice calculations with nonlinear (chiral) pion mass extrapolations, with chiral effective field theory, and with dynamical models with pion cloud effects. These results confirm the dominance, and general Q^2 variation, of the pionic contribution at large distances.

PACS. 13.60.Le Meson production – 13.40.Gp Electromagnetic form factors – 14.20.Gk Baryon resonances with $S = 0$

Experimental confirmation of the presence of nonspherical hadron amplitudes (*i.e.* d states in quark models or p-wave π-N states) is fundamental and has been the subject of intense experimental and theoretical interest (for reviews see [1–3]). This effort has focused on the measurement of the electric and Coulomb quadrupole amplitudes ($E2, C2$) in the predominantly $M1$ (magnetic dipole-quark spin flip) $\gamma^*N \to \Delta$ transition. Measurements of the $E2$ amplitude from photopion reaction experiments with polarized photons have been reported [4,5]. Electroproduction experiments at JLab [6, 7] for Q^2 from 0.4 to 4.0 $(\mathrm{GeV}/c)^2$, at Bates [8–11] at $Q^2 = 0.127$ $(\mathrm{GeV}/c)^2$ and Mainz [12–14] at $Q^2 = 0.127, 0.20$ $(\mathrm{GeV}/c)^2$ have been published. The present result at $Q^2 = 0.060$ $(\mathrm{GeV}/c)^2$ is the lowest-Q^2 value probed to date in modern, precision electroproduction. It adds a very important point to determine the physical basis of long-range nucleon and Δ nonspherical amplitudes and is a test of the Q^2 region where pionic effects are predicted to be dominant and appreciably changing.

[a] *Current address*: Department of Physics, Duke University/TUNL, Durham, NC 27708, USA.
[b] *Current address*: Radiation Laboratory, RIKEN, 2-1 Hirosawa, Wako, Saitama 351-0198, Japan.
[c] e-mail: `bernstein@lns.mit.edu` (corresponding author)
[d] *Current address*: Universität Bonn, Physikalisches Institut, Nussallee 12, D-53115 Bonn, Germany.

Since the proton has spin 1/2, no quadrupole moment can be measured. However, the Δ has spin 3/2 so the $\gamma^* N \rightarrow \Delta$ reaction can be studied for quadrupole amplitudes in the nucleon and Δ. Due to spin and parity conservation in the $\gamma^* N(J^\pi = 1/2^+) \rightarrow \Delta(J^\pi = 3/2^+)$ reaction, only three multipoles can contribute to the transition: the magnetic dipole ($M1$), the electric quadrupole ($E2$), and the Coulomb quadrupole ($C2$) photon absorption multipoles. The corresponding resonant pion production multipoles are $M_{1+}^{3/2}$, $E_{1+}^{3/2}$, and $S_{1+}^{3/2}$. The relative quadrupole to dipole ratios are EMR = $\mathrm{Re}(E_{1+}^{3/2}/M_{1+}^{3/2})$ and CMR = $\mathrm{Re}(S_{1+}^{3/2}/M_{1+}^{3/2})$. In the quark model, the nonspherical amplitudes in the nucleon and Δ are caused by the noncentral, tensor interaction between quarks [15]. However, the magnitudes of this effect for the predicted $E2$ and $C2$ amplitudes [16] are at least an order of magnitude too small to explain the experimental results (see fig. 3 below) and even the dominant $M1$ matrix element is $\simeq 30\%$ low [3,16]. A likely cause of these dynamical shortcomings is that the quark model does not respect chiral symmetry, whose spontaneous breaking leads to strong emission of virtual pions (Nambu-Goldstone bosons) [3]. These couple to nucleons as $\vec{\sigma} \cdot \vec{p}$ where $\vec{\sigma}$ is the nucleon spin, and $\vec{p}$ is the pion momentum. The coupling is strong in the p-wave and mixes in nonzero angular-momentum components. Based on this, it is physically reasonable to expect that the pionic contributions increase the $M1$ and dominate the $E2$ and $C2$ transition matrix elements in the low-Q^2 (large distance) domain. This was first indicated by adding pionic effects to quark models [17], subsequently shown in pion cloud model calculations [18,19], and recently demonstrated in chiral effective field theory calculations [20,21].

The five-fold differential cross-section for the $p(\vec{e}, e'p)\pi^0$ reaction is written as five two-fold differential cross-sections with an explicit ϕ^*-dependence as [22]

$$\frac{\mathrm{d}^5\sigma}{\mathrm{d}\Omega_f \mathrm{d}E_f \mathrm{d}\Omega} = \Gamma(\sigma_T + \epsilon\sigma_L + v_{LT}\sigma_{LT}\cos\phi^* + \epsilon\sigma_{TT}\cos 2\phi^* + h p_e v_{LT'}\sigma_{LT'}\sin\phi^*), \quad (1)$$

where ϵ is the transverse polarization of the virtual photon, $v_{LT} = \sqrt{2\epsilon(1+\epsilon)}$, $v_{LT'} = \sqrt{2\epsilon(1-\epsilon)}$, Γ is the virtual photon flux, ϕ^* is the pion center-of-mass azimuthal angle with respect to the electron scattering plane, h is the electron helicity, and p_e is the magnitude of the electron longitudinal polarization. The virtual photon differential cross-sections $(\sigma_T, \sigma_L, \sigma_{LT}, \sigma_{TT}, \sigma_{LT'})$ are all functions of the center-of-mass energy W, the four-momentum transfer squared Q^2, and the pion center-of-mass polar angle $\theta_{\pi q}^*$ (measured from the momentum transfer direction). They are bilinear combinations of the multipoles [22].

The $p(\vec{e}, e'p)\pi^0$ measurements were performed using the A1 spectrometers at the Mainz microtron [23]. Electrons were detected in spectrometer A and protons in spectrometer B. Timing and missing-mass cuts were sufficient to eliminate the π^- background. Spectrometer B has the ability to measure at up to 10 degrees out-of-plane in the lab. Due to the Lorentz boost this is significantly larger in the center-of-mass frame. The Mainz microtron delivers a longitudinally polarized, continuous, 855 MeV beam. Beam polarization was measured periodically with a Møller polarimeter to be $\approx 75\%$. The beam of up to 25 μA was scattered from a liquid-hydrogen cryogenic target. Sequential measurements were made at $W =$ 1221 MeV, $Q^2 = 0.060$ GeV$^2/c^2$, and $\theta_{\pi q}^* = 143, 156, 180^\circ$. For nonparallel measurements ($\theta_{\pi q}^* \neq 180$), the proton arm was moved through three ϕ^* settings while keeping the $\theta_{\pi q}^*$ value constant. The spectrometers were aligned in the lab with a precision of 0.6 mm and 0.1 mrad with a central momentum resolution of 0.01% and angular resolution at the target of 3 mrad [23]. The beam energy has an absolute uncertainty of ± 160 keV and a spread of 30 keV (FWHM) [23]. The effects of these uncertainties and the various kinematic cuts were studied to estimate an overall systematic error for the cross-sections of 3 to 4%. This was tested with elastic electron-proton scattering and the data agree with a fit to the world data [24] at the 3% level.

With measurements at three $\phi_{\pi q}^*$ values at a fixed $\theta_{\pi q}^*$ and using a polarized electron beam, the cross-sections $\sigma_0 = \sigma_T + \epsilon\sigma_L, \sigma_{TT}, \sigma_{LT}$, and $\sigma_{LT'}$ can be extracted from the ϕ^* and beam helicity dependence of the cross-section. Care was taken to ensure good kinematic overlap between the different angular settings. Typically, the phase space overlaps were $\Delta W \approx 40$ MeV, $\Delta Q^2 \approx 0.04$ GeV$^2/c^2$, $\Delta\theta_{\pi q}^* \approx 10^\circ$, and $\Delta\phi_{\pi q}^* \approx 40^\circ$. Since the cross-sections vary across the spectrometer acceptance, the shape of the cross-section given by several models was used to refer all of the points to the center of the acceptance. This is a small correction (typically 3%) and depends only on the relative cross-sections across the spectrometer acceptance. Several models were used for the collapse and each gives results consistent at the 0.5% level [25].

The measured partial cross-sections are plotted in figs. 1 and 2. Figure 1 shows σ_0 and σ_{LT} with the chiral effective field theory (EFT) predictions [21] which have uncertainties which reflect an estimate of the neglected higher-order terms in the chiral expansion. The other models are the phenomenological model MAID 2003 [26], the pion cloud dynamical models of Sato and Lee [18] and of DMT [19] (Dubna, Mainz, and Taipei), and the SAID multipole analysis [27]. There is a significant spread in these model calculations due to differences in the resonant and background amplitudes. However, it is impressive that the four model curves almost fall on top of each other when the three resonant $\gamma^* p \rightarrow \Delta$ amplitudes $(M_{1+}^{3/2}, E_{1+}^{3/2}, S_{1+}^{3/2})$ are varied to fit the data as shown in the lower panel of fig. 1. In addition, this panel shows the "spherical" calculated curves when the resonant quadrupole amplitudes ($E_{1+}^{3/2}$ in σ_0 and $S_{1+}^{3/2}$ in σ_{LT}) are set equal to zero. The difference between the spherical and full curves shows the sensitivity of these cross-sections to the quadrupole amplitudes and demonstrates the basis of the present measurement. The small spread in the spherical curves indicates their sensitivity to the model dependence of the background amplitudes.

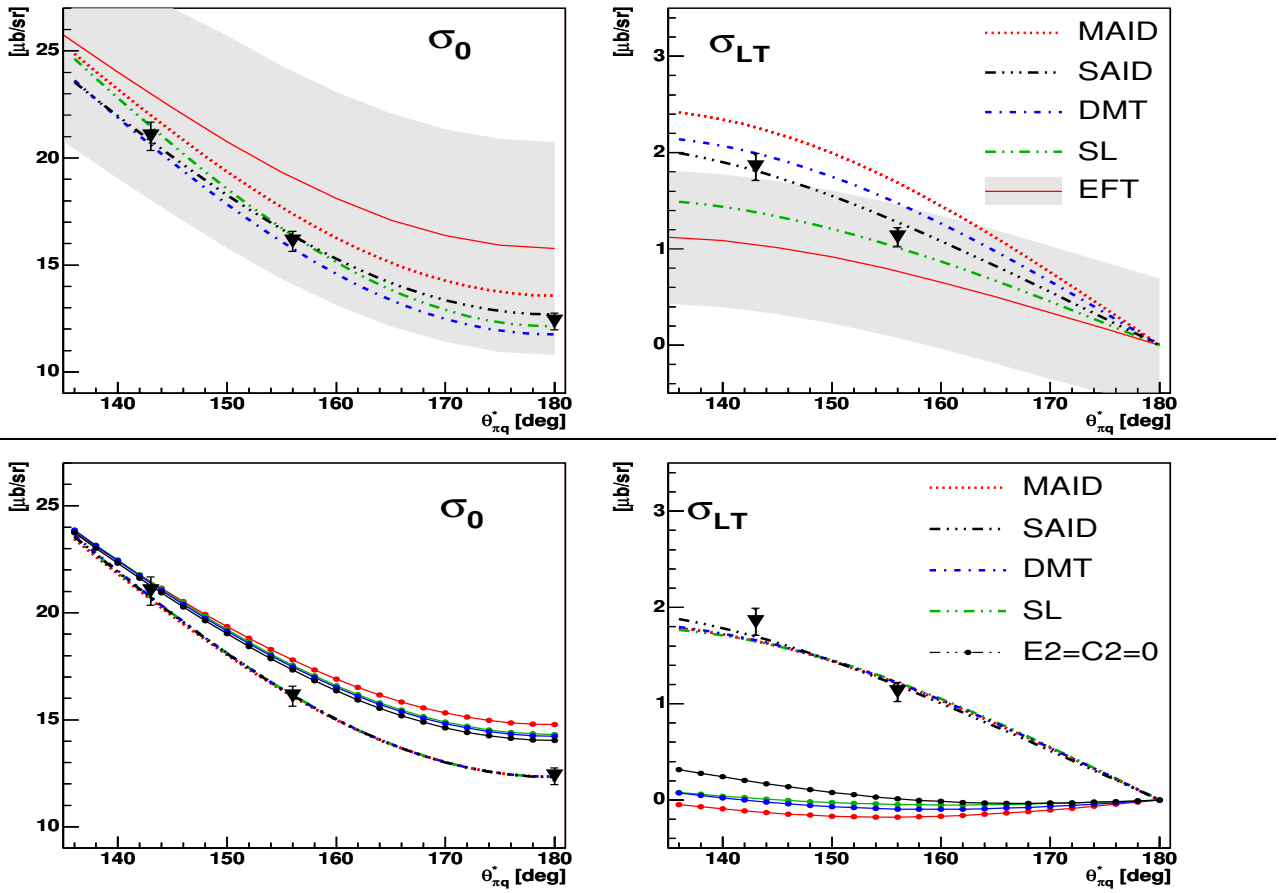

Fig. 1. (Color online) The measured $\sigma_0 = \sigma_T + \epsilon\sigma_L$ and σ_{LT} differential cross-sections as a function of $\theta^*_{\pi q}$ at $W = 1221$ MeV and $Q^2 = 0.060$ (GeV/c)^2 before (top panels) and after (bottom panels) fitting. The ▼ symbols are our data points and include the experimental and model errors (see table 1) added in quadrature. The EFT predictions [21] are plotted with their estimated uncertainties. The other curves represent predictions from the MAID 2003 [26], SL (Sato-Lee) [18], DMT [19], and SAID [27] models. The lines with dots are the fitted models with the $E^{3/2}_{1+}$ and $S^{3/2}_{1+}$ quadrupole terms set to zero.

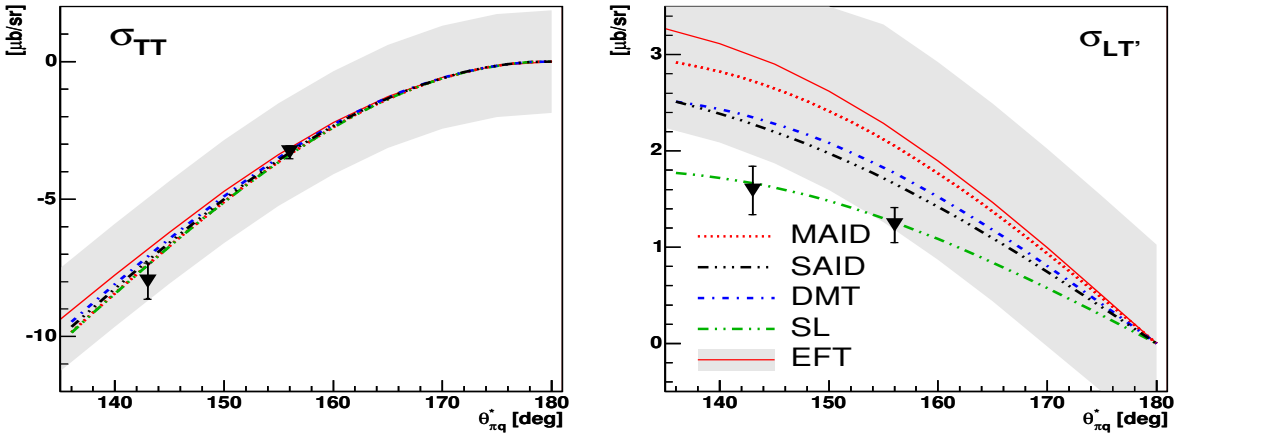

Fig. 2. (Color online) The measured σ_{TT} and $\sigma_{LT'}$ differential cross-sections as a function of $\theta^*_{\pi q}$ at $W = 1221$ MeV and $Q^2 = 0.060$ (GeV/c)^2. The ▼ symbols are our data points and include the experimental and model errors (see table 1) added in quadrature. The EFT predictions [21] are plotted with their estimated uncertainties. The other curves represent predictions from the MAID 2003 [26], SL (Sato-Lee) [18], DMT [19], and SAID [27] models. The model curves after fitting are almost identical to those before and so have been suppressed. See text for details.

Table 1. Values of EMR(%), CMR(%), and $M_{1+}^{3/2}$ (in $10^{-3}/m_{\pi^+}$) extracted from these data with three resonant parameter fits using the SAID [27], MAID 2003 [26], Sato-Lee (SL) [18], and DMT [19] models at the Δ-resonance, $W = 1232$ MeV, at $Q^2 = 0.060$ (GeV/c)^2. The original model predictions are in square brackets. The first error is the statistical and cut errors added in quadrature. For $M_{1+}^{3/2}$ the second error is the systematic error (for the EMR and CMR they are negligible). For the average, the third error is the model error defined as the RMS deviation of the results from the four different models. The bottom two lines are the EFT predictions of Gail and Hemmert (GH) [20] and Pascalutsa and Vanderhaeghen (PV) [21].

	EMR (%)	CMR (%)	$M_{1+}^{3/2}$
SAID	$-2.18 \pm 0.31\,[-1.80]$	$-4.87 \pm 0.29\,[-5.30]$	$40.81 \pm 0.29 \pm 0.57\,[40.72]$
SL	$-2.26 \pm 0.30\,[-2.98]$	$-4.46 \pm 0.25\,[-3.48]$	$40.20 \pm 0.27 \pm 0.56\,[41.28]$
DMT	$-2.11 \pm 0.28\,[-2.84]$	$-4.85 \pm 0.26\,[-5.74]$	$40.78 \pm 0.27 \pm 0.57\,[40.81]$
MAID	$-2.56 \pm 0.27\,[-2.16]$	$-5.07 \pm 0.26\,[-6.51]$	$39.51 \pm 0.26 \pm 0.57\,[40.53]$
Avg.	$-2.28 \pm 0.29_{\rm stat+sys} \pm 0.20_{\rm model}$	$-4.81 \pm 0.27_{\rm stat+sys} \pm 0.26_{\rm model}$	$40.33 \pm 0.27_{\rm stat} \pm 0.57_{\rm sys} \pm 0.61_{\rm model}$
GH	-2.66	-6.06	41.15
PV	-2.88 ± 0.70	-5.85 ± 1.40	39.75 ± 3.87

Figure 2 shows the measured cross-sections for σ_{TT} and $\sigma_{LT'}$ with the same model curves as in fig. 1. It is seen that within the relatively large estimated uncertainties the chiral effective field theory calculations [21] are consistent with experiment. For σ_{TT} the four model calculations [26, 18,19,27] are in good agreement with each other and with the data. However, for $\sigma_{LT'}$ this is not the case and only the Sato-Lee model agrees with experiment.

It is instructive to examine why σ_{LT} is sensitive to the Coulomb quadrupole amplitude, Im$[S_{1+}]$, and $\sigma_{LT'}$ is primarily sensitive to the background. The time reversal even observable σ_{LT} contains the interference amplitude Re$[S_{1+}^* M_{1+}]$ which is primarily sensitive to Im$[S_{1+}]$Im$[M_{1+}]$ where the latter is the dominant multipole amplitude. By contrast, the time reversal odd observable $\sigma_{LT'}$ contains Im$[S_{1+}^* M_{1+}]$. This is primarily sensitive to Re$[S_{1+}]$Im$[M_{1+}]$ and therefore does not measure the Coulomb quadrupole amplitude but rather is sensitive to a background term times the dominant magnetic dipole term. The details will be presented in a future publication [28].

On the other hand, the other cross-sections show a minimum of model dependence and can be used to accurately extract the three resonant amplitudes as will be discussed below. The model curves after fitting for σ_{TT} and $\sigma_{LT'}$ are almost identical to those before and so have been suppressed. $\sigma_{LT'}$ is insensitive to the resonant parameters, as mentioned above, and σ_{TT}, while sensitive to E_{1+}, is dominated by the M_{1+} term.

As has been discussed above, we have obtained the values of the three resonance amplitudes $(M_{1+}^{3/2}, E_{1+}^{3/2}, S_{1+}^{3/2})$ using fits with four reaction models [26,18,19,27]. Correlations between the fitting parameters were taken into account in the errors estimated by the fitting routine [25, 29]. The fits were performed using the spectrometer cross-sections and were the same (within the errors) whether or not the $\sigma_{LT'}$ data were included. In addition, the fits used the entire $I = 3/2$ amplitude so that the unitarity of each model was preserved. At resonance, these $I = 3/2$ amplitudes are purely imaginary due to the Fermi-Watson theorem [22]. The fits were performed at the same value of W at which the data were taken. The models were then used to extrapolate the value of the multipoles at $W = 1232$ MeV. Following our previous work [2,11] we took the final results to be the average of these model determinations and estimated the model-dependent error in the resonance amplitudes by taking the RMS deviation of the values [25]. We believe that this is reasonable since the chosen models represent state-of-the-art calculations and also a variety of different approaches. The results of the fits for the resonant multipoles along with the EFT predictions are presented in table 1 along with the original values for several models. We also present the average fitted values for the four reaction models considered here. The differences between these values represent the model dependence due to the different background multipoles. The effect of background amplitudes on the resonant amplitudes was studied and determined to have an effect approximately the same size as the model to model RMS deviation. This study is detailed in refs. [25] and [28]. For the result of this experiment we take the average values of the fitted multipoles using each model along with both the experimental and model error. It can be seen that the model and experimental errors are approximately the same magnitude. There is generally good agreement between the EFT predictions and our experimental results. This also indicates the importance of the pion contribution to these amplitudes. It can also be seen from table 1 that the dispersion between the original model calculations for the quadrupole amplitudes has been considerably reduced by the fitting. For the EMR the RMS deviation in the original models is reduced from 0.56% to 0.20%. For the CMR the RMS deviation in the original models is reduced even more, from 0.82% to 0.26%.

Figure 3 shows the evolution of the multipole ratios at low Q^2. There is reasonable consistency of the results from the different laboratories. The plotted lattice QCD results, with a linear pion mass extrapolation [30], are in general agreement with the data for the EMR but disagree for the CMR by a wide margin. The EFT analysis of Pascalutsa and Vanderhaeghen (PV) [21] indicates that a linear extrapolation is close to the data for the

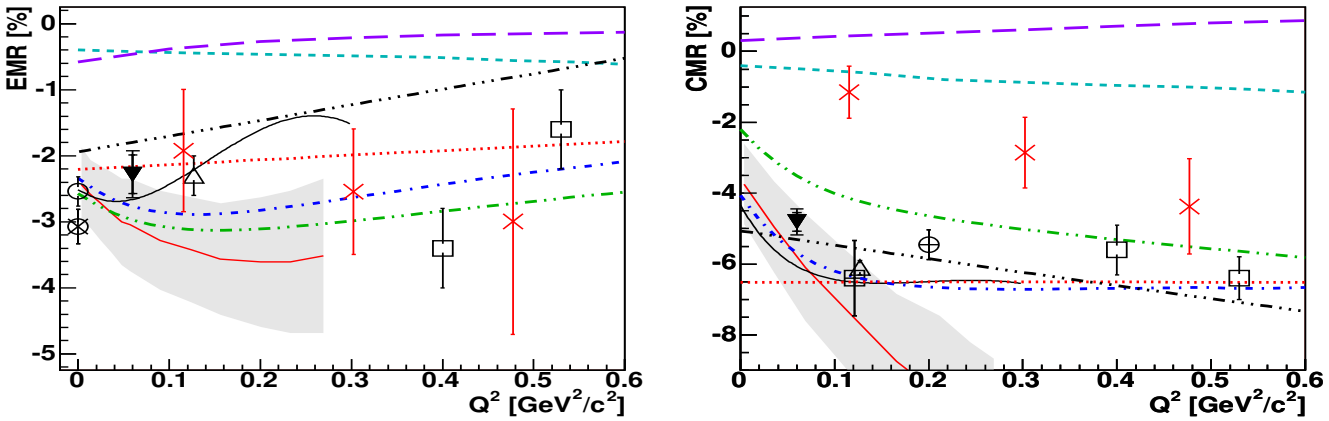

Fig. 3. (Color online) The low-Q^2-dependence of the EMR and CMR at $W = 1232$ MeV for the $\gamma^* p \to \Delta$ reaction. The ▼ symbols are our data points and include the experimental and model errors (see table 1) added in quadrature. The other data are: the photon point ◯ [4] and ⊗ [5]; CLAS, □ [6]; Bates, △ [11]; Elsner, ⊕ [14] and Pospischil, ⊞ [12]. The lattice QCD calculations with linear pion mass extrapolations are shown as × [30] and also the recent chiral perturbation calculations of Pascalutsa and Vanderhaeghen (PV) (see EFT in fig. 1) [21] and Gail and Hemmert (GH) (black solid line) [20]. The other curves represent the same models as in fig. 1. The HQM (long-dashed line) [31] and Capstick (short-dashed line) [16] quark models have been included.

EMR but results in a considerable underestimation of the CMR. The results of the two chiral calculations [20,21] are also presented in fig. 3. As these are effective field theories they contain empirical low-energy constants. For Gail and Hemmert this includes fits to the dominant $M_{1+}^{3/2}$ multipole for $Q^2 \leq 0.2$ $(\mathrm{GeV}/c)^2$ and for the EMR at the photon point ($Q^2 = 0$). In order to achieve the good overall agreement they had to employ one higher-order term with another empirical constant. As also can be seen from the large estimated errors of the Pascalutsa and Vanderhaeghen EFT calculation [21] a treatment of the next higher-order term is required. In fig. 3 two representative constituent quark models, the newer hypercentral quark model (HQM) [31], and an older nonrelativistic calculation of Capstick [16], have been included (the relativistic calculations are in even worse agreement with experiment). These curves are representative of quark models which typically under-predict the dominant $M_{1+}^{3/2}$ multipole by $\simeq$ 30% and underestimate the EMR and CMR by an order of magnitude, even predicting the wrong sign. One solution to this problem has been to add pionic degrees of freedom to quark models [17]. All of these models treat the Δ as a bound state and therefore do not have the πN continuum (*i.e.*, no background amplitudes) so that cross-sections are not calculated. The Sato-Lee [18] and DMT [19] dynamical reaction models with pion cloud effects bridge this gap and are in qualitative agreement with the Q^2 evolution of the data. These models calculate the virtual pion cloud contribution dynamically but have an empirical parameterization of the inner (quark) core contribution which gives them some flexibility in these observables. By contrast the empirical MAID [26] and SAID [27] represent fits to other data with a smooth Q^2-dependence.

One way to see the major role played by the pion cloud contribution to the resonant multipoles is that for this case the expected scale for the Q^2 evolution is $m_\pi^2 = 0.02\,\mathrm{GeV}^2$. In these units the range of the present experiment from Q^2 from 0.060 to $0.20\,\mathrm{GeV}^2/c^2$ is 3 to 10 units. Therefore it is not surprising that one should see relatively large changes in the predicted Q^2 evolution of the resonant multipoles as is shown in fig. 3. It is also clear that there is significant model dependence in these predictions.

In conclusion, the new data are at the lowest measured Q^2 for modern electroproduction where the dominant pionic contribution is predicted to be increasing. This Q^2 region is sufficiently low to be able to test chiral effective calculations. These results are in qualitative agreement with lattice calculations with a chiral extrapolation to the physical pion mass [21], with recent chiral perturbation theory calculations [20,21] and with dynamical models which explicitly include the pion cloud [18,19]. However, all of these calculations require refinements in order to obtain quantitative agreement with experiment. This includes lattice calculations with lighter pion masses and the next order in effective field theory.

We thank L. Tiator, D. Drechsel, T.-S.H. Lee, V. Pascalutsa, M. Vanderhaeghen, T. Gail and T. Hemmert for their assistance with valuable discussions and for sharing their unpublished work. This work is supported at Mainz by the Sonderforschungsbereich 443 of the Deutsche Forschungsgemeinschaft (DFG), University of Athens by the Program PYTHAGORAS of the Greek ministry of Education (co-funded by the European Social Fund and National Resources), and at MIT by the U.S. DOE under Grant No. DE-FG02-94ER40818.

References

1. D. Drechsel, L. Tiator (Editors), *Proceedings of the Workshop on the Physics of Excited Nucleons* (World Scientific, 2001).
2. C.N. Papanicolas, Eur. Phys. J. A **18**, 141 (2003).

3. A.M. Bernstein, Eur. Phys. J. A **17**, 349 (2003).
4. R. Beck *et al.*, Phys. Rev. C **61**, 035204 (2000).
5. G. Blanpied *et al.*, Phys. Rev. C **64**, 025203 (2001).
6. K. Joo *et al.*, Phys. Rev. Lett. **88**, 122001 (2002).
7. V.V. Frolov *et al.*, Phys. Rev. Lett. **82**, 45 (1999).
8. G.A. Warren *et al.*, Phys. Rev. C **58**, 3722 (1998).
9. C. Mertz *et al.*, Phys. Rev. Lett. **86**, 2963 (2001).
10. C. Kunz *et al.*, Phys. Lett. B **564**, 21 (2003).
11. N.F. Sparveris *et al.*, Phys. Rev. Lett. **94**, 022003 (2005).
12. T. Pospischil *et al.*, Phys. Rev. Lett. **86**, 2959 (2001).
13. P. Bartsch *et al.*, Phys. Rev. Lett. **88**, 142001 (2002).
14. D. Elsner *et al.*, Eur. Phys. J. A **27**, 91 (2006).
15. S.L. Glashow, Physica A **96**, 27 (1979).
16. S. Capstick, G. Karl, Phys. Rev. D **41**, 2767 (1990).
17. D.H. Lu, A.W. Thomas, A.G. Williams, Phys. Rev. C **55**, 3108 (1997); U. Meyer, E. Hernandez, A.J. Buchmann, Phys. Rev. C **64**, 035203 (2001); M. Fiolhais, B. Golli, S. Sirca, Phys. Lett. B **373**, 229 (1996).
18. T. Sato, T.S.H. Lee, Phys. Rev. C **63**, 055201 (2001).
19. S.S. Kamalov *et al.*, Phys. Lett. B **522**, 27 (2001).
20. T.A. Gail, T.R. Hemmert, `nucl-th/0512082` (2005).
21. V. Pascalutsa, M. Vanderhaeghen, Phys. Rev. Lett. **95**, 232001 (2005).
22. D. Drechsel, L. Tiator, J. Phys. G **18**, 449 (1992).
23. K.I. Blomqvist *et al.*, Nucl. Instrum. Methods A **403**, 263 (1998).
24. P. Mergell, U.G. Meissner, D. Drechsel, Nucl. Phys. A **596**, 367 (1996).
25. S. Stave, PhD Dissertation, MIT (2006) (unpublished).
26. D. Drechsel, O. Hanstein, S.S. Kamalov, L. Tiator, Nucl. Phys. A **645**, 145 (1999).
27. R.A. Arndt *et al.*, Phys. Rev. C **66**, 055213 (2002) `http://gwdac.phys.gwu.edu`.
28. S. Stave *et al.*, to be published in the *Proceedings of the Workshop on the Shape of Hadrons, Athens, Greece, 27-29 Apr 2006*, edited by C.N. Papanicolas, A.M. Bernstein (AIP).
29. F. James, M. Roos, Comput. Phys. Commun. **10**, 343 (1975).
30. C. Alexandrou *et al.*, Phys. Rev. Lett. **94**, 021601 (2005).
31. M. De Sanctis *et al.*, Nucl. Phys. A **755**, 294 (2005).